

# Synthesis and Structural Characterization of the Bis(diisopropylamino)boron Enolate of *tert*-Butyl Methyl Ketone

Lili Ma,<sup>†</sup> Russell Hopson,<sup>†</sup> Deyu Li,<sup>†</sup> Yong Zhang,<sup>‡</sup> and Paul G. Williard\*,<sup>†</sup>

Department of Chemistry, Brown University, Providence, Rhode Island 02912 and Department of Chemistry, Boston University, 590 Commonwealth Avenue, Boston, Massachusetts 02215

Received July 5, 2007

Lithium, sodium, and potassium enolates reacted with bisaminoboron halides to give bisaminoboron enolates **1a–5c**. Specifically, the potassium enolate of *tert*-butyl methyl ketone reacted with bis(diisopropylamino)boron chloride in THF at room temperature within 1 h to give the bis(diisopropylamino)boron enolate of *tert*-butyl methyl ketone (**3b**) in 61–84% isolated yields. Under similar conditions, the reactivity is highly dependent on the metal employed to generate enolates (K > Na > Li) as well as the nitrogen substituents in the bisaminoboron halides (iPr > Et > TMS). This latter observation is a compromise between the boron–nitrogen resonance and the steric effect. The structural information of enolate **3b** was studied in detail. Unlike the aggregated alkali-metal enolates, this boron enolate exists exclusively as a monomer in both the solid and solution states, as identified by X-ray and diffusion-ordered NMR.

## Introduction

Boron enolates enjoy widespread use in synthetic organic chemistry due to the relatively mild conditions used to generate these intermediates and the stereoselectivity observed in both the enolization reaction and the subsequent aldol reactions.<sup>1</sup> The most widely utilized asymmetric synthetic methodology involving boron enolates developed from the extensive studies of Evans and co-workers beginning 30 years ago.<sup>2</sup> H. C. Brown also reported extensively on the stereoselectivity of enolboration and aldol reaction of the corresponding boron enolates starting from dialkyl boron halides.<sup>3</sup> In light of our previous structural characterizations of Li, Na, K, and Mg enolates of simple ketones<sup>4</sup> and the dearth of structural information on simple boron enolates,<sup>5</sup> we report the preparation of several bisaminoboron

Table 1. Conditions for Bisaminoboron Enolates from Bisaminoboron Chlorides and Metal Enolates

|           |                      | Metal                                      | T(°C) | t(h) | Yield(%) <sup>a</sup> |    |
|-----------|----------------------|--|-------|------|-----------------------|----|
|           | <b>1a</b>            | R <sub>1</sub> = Et, R <sub>2</sub> = H    | K     | 25   | 1                     | 53 |
|           | <b>1b</b>            | R <sub>1</sub> = iPr, R <sub>2</sub> = H   | K     | 25   | 1                     | 98 |
|           | <b>1c</b>            | R <sub>1</sub> = TMS, R <sub>2</sub> = H   | K     | 60   | 12                    | 90 |
|           | <b>2a</b>            | R <sub>1</sub> = Et, R <sub>2</sub> = tBu  | K     | 25   | 1                     | 59 |
|           | <b>2b</b>            | R <sub>1</sub> = iPr, R <sub>2</sub> = tBu | K     | 25   | 1                     | 96 |
|           | <b>2c</b>            | R <sub>1</sub> = TMS, R <sub>2</sub> = tBu | K     | 60   | 12                    | 94 |
|           | <b>3a</b>            | R <sub>1</sub> = Et                        | K     | 25   | 2                     | 88 |
|           | <b>3b</b>            | R <sub>1</sub> = iPr                       | Li    | 60   | 24                    | 56 |
|           | <b>3b</b>            | R <sub>1</sub> = iPr                       | Na    | 25   | 1                     | 92 |
|           | <b>3b</b>            | R <sub>1</sub> = iPr                       | K     | 25   | 1                     | 99 |
|           | <b>3c</b>            | R <sub>1</sub> = TMS                       | Li    | 60   | 24                    | 12 |
|           | <b>3c</b>            | R <sub>1</sub> = TMS                       | Na    | 60   | 4                     | 77 |
| <b>3c</b> | R <sub>1</sub> = TMS | K  | 60    | 2    | 91                    |    |
|           | <b>4a</b>            | R <sub>1</sub> = Et                        | K     | 25   | 2                     | 81 |
|           | <b>4b</b>            | R <sub>1</sub> = iPr                       | K     | 25   | 1                     | 98 |
|           | <b>4c</b>            | R <sub>1</sub> = TMS                       | K     | 60   | 2                     | 90 |
|           | <b>5a</b>            | R <sub>1</sub> = Et                        | K     | 25   | 2                     | 78 |
|           | <b>5b</b>            | R <sub>1</sub> = iPr                       | K     | 25   | 1                     | 94 |
|           | <b>5c</b>            | R <sub>1</sub> = TMS                       | K     | 60   | 2                     | 40 |

<sup>a</sup> Yields before recrystallization. Their purity was confirmed by <sup>1</sup>H and <sup>11</sup>B NMR spectra.

enolates derived from simple ketones and the crystal structure of the bis(diisopropylamino)boron enolate of *tert*-butyl methyl ketone.

## Results and Discussion

**Synthesis of Bisaminoboron Enolates.** As is true for many aldol reactions, the role of boron enolates is often crucial. As a starting point to study the mechanism of boron-mediated reactions, we concentrate our investigation on the boron enolates listed in Table 1, a compound class that performs aldol-type and Mannich-type reactions with aldehydes. These compounds

\* To whom correspondence should be addressed. Fax: 01-401-863-9368. E-mail: pgw@brown.edu.

<sup>†</sup> Brown University, Providence.

<sup>‡</sup> Boston University, Boston.

(1) (a) Ishihara, K.; Yamamoto, H. *Modern Aldol Reactions*; Wiley-VCH Verlag GmbH: Weinheim, FRG, 2004; Vol. 2, pp 25–68. (b) Mukaiyama, T.; Matsuo, J.-I. *Modern Aldol Reactions*; Wiley-VCH Verlag GmbH: Weinheim, FRG, 2004; Vol. 1, pp 127–160. (c) Cowden, C. J.; Paterson, I. *Organic Reactions*; John Wiley & Sons: New York, 1997; Vol. 51, pp 1–200.

(2) (a) Evans, D. A.; Cote, B.; Coleman, P. J.; Connell, B. T. *J. Am. Chem. Soc.* **2003**, *125*, 10893. (b) Duffy, J. L.; Yoon, T. P.; Evans, D. A. *Tetrahedron Lett.* **1995**, *36*, 9245. (c) Evans, D. A.; Nelson, J. V.; Vogel, E.; Taber, T. R. *J. Am. Chem. Soc.* **1981**, *103*, 3099. (d) Evans, D. A.; Bartroli, J.; Shih, T. L. *J. Am. Chem. Soc.* **1981**, *103*, 2127. (e) Evans, D. A.; Taber, T. R. *Tetrahedron Lett.* **1980**, *21*, 4675. (f) Evans, D. A.; Vogel, E.; Nelson, J. V. *J. Am. Chem. Soc.* **1979**, *101*, 6120. (g) Evans, D. A.; Thomas, R. C.; Walker, J. A. *Tetrahedron Lett.* **1976**, 1427. (h) Evans, D. A.; Crawford, T. C.; Thomas, R. C.; Walker, J. A. *J. Org. Chem.* **1976**, *41*, 3947.

(3) (a) Ramachandran, P. V.; Zou, M.-F.; Brown, H. C. *Helv. Chim. Acta* **2002**, *85*, 3027. (b) Ganesan, K.; Brown, H. C. *J. Org. Chem.* **1994**, *59*, 7346. (c) Ganesan, K.; Brown, H. C. *J. Org. Chem.* **1993**, *58*, 7162. (d) Ganesan, K.; Brown, H. C. *J. Org. Chem.* **1994**, *59*, 2336. (e) Brown, H. C.; Ganesan, K.; Dhar, R. K. *J. Org. Chem.* **1993**, *58*, 147. (f) Brown, H. C.; Ganesan, K.; Dhar, R. K. *J. Org. Chem.* **1992**, *57*, 3767. (g) Brown, H. C.; Dhar, R. K.; Ganesan, K.; Singaram, B. *J. Org. Chem.* **1992**, *57*, 2716. (h) Brown, H. C.; Dhar, R. K.; Ganesan, K.; Singaram, B. *J. Org. Chem.* **1992**, *57*, 499.

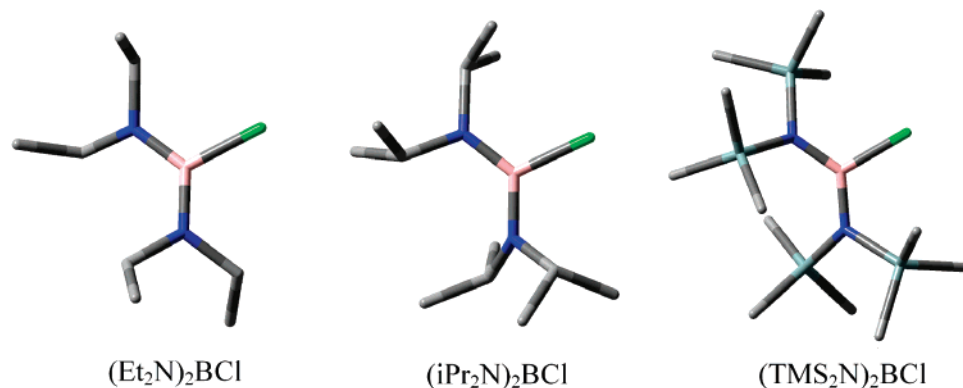


**Figure 1.** B3LYP/6-31G\*-optimized geometries of  $(\text{Et}_2\text{N})_2\text{BCl}$ ,  $(i\text{Pr}_2\text{N})_2\text{BCl}$ , and  $(\text{TMS}_2\text{N})_2\text{BCl}$ . Hydrogen atoms are omitted for clarity.

**Table 2. Selected Bond Distances, Torsion Angles, and Partial Charges for Bisaminoboron Chlorides**

| compound                | $(\text{Et}_2\text{N})_2\text{BCl}$ | $(i\text{Pr}_2\text{N})_2\text{BCl}$ | $(\text{TMS}_2\text{N})_2\text{BCl}$ |
|-------------------------|-------------------------------------|--------------------------------------|--------------------------------------|
| B(1)–N(2) (Å)           | 1.42353                             | 1.41903                              | 1.43736                              |
| B(1)–N(3) (Å)           | 1.42492                             | 1.44174                              | 1.43736                              |
| B(1)–Cl(4) (Å)          | 1.83861                             | 1.85500                              | 1.86900                              |
| Cl(4)–B(1)–N(2)–C (deg) | 17.065                              | 18.211                               | 36.685                               |
| Cl(4)–B(1)–N(3)–C (deg) | 27.645                              | 37.734                               | 36.684                               |
| B(1) (e)                | +0.378                              | +0.402                               | +0.497                               |
| N(2) (e)                | –0.357                              | –0.368                               | –0.790                               |
| N(3) (e)                | –0.362                              | –0.413                               | –0.790                               |
| Cl(4) (e)               | –0.258                              | –0.259                               | –0.258                               |

were prepared by reaction of preformed Li, Na, or K enolates of the corresponding ketones with bisaminoboron halides.<sup>6</sup> The yield of boron enolate formation is highly dependent on the alkali-metal cation in the expected order  $\text{K} > \text{Na} > \text{Li}$  and also on the substituents on nitrogen  $i\text{Pr} > \text{Et} > \text{TMS}$ . Two factors might account for the latter observation: boron–nitrogen  $\pi$  bonding and steric hindrance.

The B–N  $\pi$  bond character arises from delocalization of the nitrogen lone pair into the empty 2p orbital on boron. Several lines of evidence support a B–N  $\pi$  bonding increase in the bisaminoboron chlorides in the following order:  $(\text{TMS}_2\text{N})_2\text{BCl} < (i\text{Pr}_2\text{N})_2\text{BCl} < (\text{Et}_2\text{N})_2\text{BCl}$ . Hence, a density functional theory (DFT) study was undertaken. The optimized geometries are shown in Figure 1.

Calculated bond distances and partial charges on these atoms (B3LYP/6-31G\*) are summarized in Table 2. The two B–N bond lengths for  $(\text{Et}_2\text{N})_2\text{BCl}$  are both short with Cl–B–N–C torsion angles of about  $17.0^\circ$  and  $27.6^\circ$ , indicating formation of partial double bonds. For  $(i\text{Pr}_2\text{N})_2\text{BCl}$ , the B(1)–N(2) is short, only 1.419 Å with a  $18.2^\circ$  torsion angle, while the other is longer, 1.442 Å with a  $37.7^\circ$  torsion angle, indicating the existence of two unequal bonds. In the case of  $(\text{TMS}_2\text{N})_2\text{BCl}$ , both B–N bonds are long and both torsion angles are large. Additionally, the positive charge on B and the negative charge

on N increase with the increase of bond length. All this evidence suggests that the amount of double bond decreases with increasing steric effect.

A second yet simple piece of evidence for the B–N  $\pi$  bonding in these complexes comes from the  $^{11}\text{B}$  chemical shift. In similar structures, higher field chemical shifts are indicative of stronger resonance interaction.<sup>7</sup> The  $^{11}\text{B}$  spectra for  $(\text{TMS}_2\text{N})_2\text{BCl}$ ,  $(i\text{Pr}_2\text{N})_2\text{BCl}$ , and  $(\text{Et}_2\text{N})_2\text{BCl}$  shift upfield,  $-32.0$ ,  $-30.2$ , and  $-27.9$  ppm, respectively, as the resonance effect increases.

As the B–N  $\pi$  bond character decreases in the order  $(\text{Et}_2\text{N})_2\text{BCl} > (i\text{Pr}_2\text{N})_2\text{BCl} > (\text{TMS}_2\text{N})_2\text{BCl}$ , the Lewis acidity on boron increases and the reactivity increases correspondingly. Alternatively, as the steric hindrance of the nitrogen substituents increases in the order  $(\text{Et}_2\text{N})_2\text{BCl} < (i\text{Pr}_2\text{N})_2\text{BCl} < (\text{TMS}_2\text{N})_2\text{BCl}$ , the accessibility of boron to nucleophiles decreases and the reactivity decreases correspondingly. On the basis of this reasoning, the substituent effects observed in Table 1 were interpreted as the interplay of steric effects and B–N  $\pi$  bonding. The steric effect is more important than the  $\pi$  bonding effect since the TMS derivatives reacted much slower and often needed elevated temperatures and longer reaction times.

**Structural Features of Enolate 3b.** In addition to the synthesis of boron enolates, we were also keen to know their structure and aggregation state. Crystals of enolate **3b**<sup>8</sup> suitable for X-ray diffraction analysis were prepared from heptane at low temperature. A computer-generated plot of this crystal structure is depicted in Figure 2,<sup>9</sup> and the related crystallographic data are summarized in Table 3.

This boron enolate is a covalent monomer unlike the corresponding alkali metal pinacolone enolates, all of which exist as ionic aggregates. Significant structural features are as follows. The B atom is trigonal planar and only 0.03 Å above the plane formed by N(1), N(2), and O. A torsion angle of approximately  $18^\circ$  is observed for B–O–C(2)–C(1). Both nitrogen atoms are also relatively planar; however, there is an observable difference in the two B–N bond lengths. These bond lengths correlate to an observable difference in dihedral angles. Hence, the shorter B–N(1) bond, 1.417 Å, is associated with a

(4) (a) Sun, C.; Williard, P. G. *J. Am. Chem. Soc.* **2000**, *122*, 7829. (b) Williard, P. G.; MacEwan, G. J. *J. Am. Chem. Soc.* **1989**, *111*, 7671. (c) Williard, P. G.; Hintze, M. J. *J. Am. Chem. Soc.* **1987**, *109*, 5539. (d) Williard, P. G.; Salvino, J. M. *J. Chem. Soc., Chem. Commun.* **1986**, 153. (e) Williard, P. G.; Carpenter, G. B. *J. Am. Chem. Soc.* **1986**, *108*, 462.

(5) The closest analogs include structures reported for derivatives of oxazaborolidines: Weber, L.; Schnieder, M.; Maciel, T. C.; Wartig, H. B.; Schimmel, M.; Boese, R.; Blaeser, D. *Organometallics* **2000**, *19*, 5791. Weber, L.; Rausch, A.; Stammler, H.-G.; Neumann, B. *Z. Anorg. Allg. Chem.* **2005**, *631*, 1633. 2-Oxa-1-boranaphthalene: Arcus, V. L.; Main, L.; Nicholson, B. K. *J. Organomet. Chem.* **1993**, *460*, 139. Unpublished diphenylborane enolate: CCDC 216036.

(6) (a) Brown, H. C.; Ravindran, N. *Inorg. Chem.* **1977**, *16*, 2938. (b) Chavant, P. Y.; Vaultier, M. *J. Organomet. Chem.* **1993**, *455*, 37. (c) Geymayer, P.; Rochow, E. G. *Monatsh. Chem.* **1966**, *97*, 429.

(7) (a) Haberecht, J.; Krummland, A.; Breher, F.; Gebhardt, B.; Ruegger, H.; Nesper, R.; Gruetzmacher, H. *Dalton Trans.* **2003**, 2126. (b) Chavant, P. Y.; Vaultier, M. *J. Organomet. Chem.* **1993**, *455*, 37.

(8) A certain amount of anhydrous heptane was added to the crude product of **3b** to make a  $\sim 1.6$  M solution of boron enolate. After centrifuging briefly, the clear solution was transferred to flamed-dried glass tube and placed in a freezer at  $-50^\circ\text{C}$  during which time the boron enolate crystals formed.

(9) Crystals of **3b** were mounted on a Bruker Apex I diffractometer under a stream of dry nitrogen at  $-70^\circ\text{C}$ . Structure solution and refinement was carried out using Shelxtl programs. Crystallographic data was deposited with the Cambridge Crystallographic Data Center—#647918.

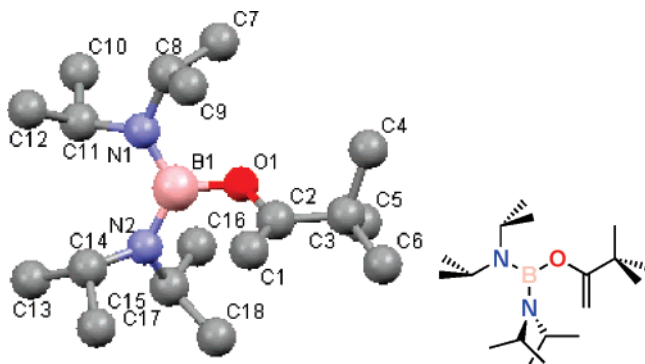


**Figure 2.** X-ray crystal structure of bis(diisopropylamino)boron enolate of pinacolone (**3b**). Hydrogen atoms are omitted for clarity. Selected bond lengths (Å) and angles (deg) with estimated standard deviations: B(1)–N(1) 1.417(2); B(1)–N(2) 1.458(2); B(1)–O(1) 1.414(2); O(1)–B(1)–N(1) 115.68(16); O(1)–B(1)–N(2) 121.71(15); N(1)–B(1)–N(2) 122.52(17).

**Table 3. Crystallographic Parameters for 3b**

|   |   |
|---|---|
| formula   | C <sub>18</sub> H <sub>39</sub> BN <sub>2</sub> O |
| fw  | 310.32  |
| cryst size (mm)   | 0.3 × 0.2 × 0.1 mm                                |
| cryst syst  | monoclinic  |
| space group   | <i>P</i> <sub>2</sub> / <i>c</i>                  |
| <i>a</i> (Å)  | 9.718(2)  |
| <i>b</i> (Å)  | 18.126(3)   |
| <i>c</i> (Å)  | 12.198(2)   |
| $\beta$ (deg)   | 109.965(3)  |
| <i>V</i> (Å <sup>3</sup> )                                  | 2019.6(6)   |
| <i>Z</i>  | 4   |
| <i>D</i> <sub>calc</sub> (g cm <sup>-3</sup> )              | 1.021   |
| $\mu$ /mm <sup>-1</sup>                                     | 0.061   |
| radiation   | Mo K $\alpha$ 0.71073                             |
| <i>T</i> /K   | 212   |
| $2\theta$ <sub>max</sub>                                    | 28.24   |
| <i>F</i> (000)  | 696   |
| <i>R</i> <sub>1</sub> ( <i>I</i> > 2 $\sigma$ ( <i>I</i> )) | 0.0669 ( <i>I</i> > 2)                            |
| w <i>R</i> <sub>2</sub> (all data)                          | 0.1764 ( <i>I</i> > 2)                            |
| goodness of fit   | 0.933   |

dihedral angle of approximately 19° between the methine C–N(2)–C plane and the N–B–N plane. A longer B–N(2) bond, 1.458 Å, is observed with a corresponding dihedral angle of nearly 48°. In the solid state, a geometry that favors overlap of the empty orbital on boron with the lone pair on N clearly leads to a shorter B–N bond length.

<sup>1</sup>H, <sup>13</sup>C, and <sup>11</sup>B NMR spectra of **3b** are shown in Figure 3. From the extensive compilation of NMR data on organoboron compounds compiled by Nöth and Wrackmeyer, trialkoxyboranes exhibit an <sup>11</sup>B chemical shift of approximately –18 ppm whereas the bis(alkyl) monoalkoxyboranes appear at about –55 ppm.<sup>10</sup> The <sup>11</sup>B chemical shift of –26 ppm (C<sub>6</sub>D<sub>6</sub> solution) for **3b** is between these two values but closer to that of a trialkoxyborane. The <sup>11</sup>B chemical shift found is identical to that reported by Suginome and Murakami for the bis(diethylamino)boron enolate of acetophenone.<sup>11</sup>

We also carried out a pulsed field gradient, diffusion-oriented NMR experiment on a solution of this enolate. Diffusion-ordered NMR spectroscopy (DOSY) has received increasing attention recently for its ability to identify reaction intermediates and aggregation status in solution.<sup>12</sup> The DOSY NMR spectrum is shown in Figure 4. On the basis of the diffusion coefficients

determined by diffusion-ordered NMR spectroscopy (DOSY), the relative ratio of the hydrodynamic radii of **3b** and the internal standard perylene is 1.186. For comparison, the geometry of these compounds was optimized by DFT calculations, and the theoretical ratio of the hydrodynamic radii was determined to be 1.155, which agrees with the experimentally derived value determined by NMR. This DOSY spectrum unambiguously indicates that **3b** exists exclusively as a monomer in solution, although dimeric aminoboranes are known.<sup>13</sup> The strong interaction of the lone pairs on the attached heteroatoms with the B precludes formation of higher aggregates.<sup>14</sup>

From the <sup>1</sup>H NMR and <sup>13</sup>C NMR spectra it can be seen that all of the isopropyl groups are equivalent at room temperature. A consequence of the relative planarity of the N, N, O, B core of this compound is the extent of bonding interaction between the B and the covalently attached heteroatoms. Additionally, it is useful to utilize dynamic NMR spectroscopy to gain insight into the rotational barriers about the B–N bonds. Corresponding studies of monoaminoboranes, R<sub>2</sub>N–BR'<sub>2</sub>, bisaminoboranes, (R<sub>2</sub>N)<sub>2</sub>–BR', and trisaminoboranes, (R<sub>2</sub>N)<sub>3</sub>B, suggest rotational barriers in the ranges of 17–24 kcal mol<sup>-1</sup>, 10–11 kcal mol<sup>-1</sup>, and complicated, correlated rotation barriers, respectively.<sup>15</sup> In all cases increasing the number and availability of lone pair electrons on covalently attached heteroatoms lowers the rotational barrier and the corresponding bond order of the B–heteroatom interaction. For enolate **3b**, we chose to monitor the methine carbon in the isopropyl group. The NMR spectra were recorded in 10 K increments from room temperature to 123 K in freon-12/THF-*d*<sub>8</sub> (80:20 v:v). A small peak begins to appear at 149 K in a ratio of 3:1 relative to a larger peak. A chemical shift difference of 302 Hz between these two peaks combined with the coalescence temperature of 159 K implies a rotational barrier of 7.05 kcal·mol<sup>-1</sup>. This value compares favorably with the values reported for bisaminoboranes.

In an attempt to explain the observed 3:1 ratio of isopropyl methine peaks in the NMR, we performed chemical shift calculations using Gaussian03. The geometry and electronic structure of the molecule were investigated at the B3LYP level with the cc-pvdz basis set. The NMR data were calculated by means of the individual gauges for atoms in molecules (IGAIM) and continuous set of gauge transformations (CSGT) methods.<sup>16</sup> The optimized geometry is in excellent agreement to the X-ray conformation. The chemical shift calculations from IGAIM and CSGT are almost identical for compound **3b**. On an absolute scale, the <sup>13</sup>C chemical shifts for the methine carbons are 139.71, 139.32, 139.28, and 138.55 ppm and the chemical shift differences between adjacent carbons are 0.39, 0.04, and 0.73 ppm. Even though these data are not calibrated, a clear trend can be seen that three methine carbons are very close to each other while the fourth methine carbon is distinguishable, leading to the observed 3:1 ratio of peaks. It is interesting to note that the distinguishable methine carbon is in the isopropyl group

(12) (a) Keresztes, I.; Williard, P. G. *J. Am. Chem. Soc.* **2000**, *122*, 10228.

(b) Schlorer, N. E.; Cabrita, E. J.; Berger, S. *Angew. Chem., Int. Ed.* **2002**, *41*, 107. (c) Cohen, Y.; Avram, L.; Frish, L. *Angew. Chem., Int. Ed.* **2005**, *44*, 520.

(13) (a) Coates, G. E.; Livingstone, J. G. *J. Chem. Soc.* **1961**, 1000. (b) Wiberg, E.; Hertwig, K.; Bolz, A. Z. *Anorg. Allg. Chem.* **1948**, *256*, 177.

(14) Lappert, M. F.; Sanger, A. R.; Srivastava, R. C.; Power, P. P. *Metal and Metalloid Amides: Synthesis, Structure, and Physical and Chemical Properties*; John Wiley & Sons: New York, 1980.

(15) (a) Beswick, Y. F.; Wisian-Neilson, P.; Neilson, R. H. *J. Inorg. Nuclear Chem.* **1981**, *43*, 2639. (b) Imbery, D.; Jaeschke, A.; Friebolin, H. *Org. Magn. Reson.* **1970**, *2*, 271. (c) Dewar, M. J. S.; Rona, P. *J. Am. Chem. Soc.* **1969**, *91*, 2259.

(16) (a) Baldrige, K. K.; Siegel, J. S. *J. Phys. Chem. A* **1999**, *103*, 4038.

(b) Huang, M.-J.; Lee, K. S. *Mol. Phys.* **2005**, *103* (15–16), 2229.

(10) Noeth, H.; Wrackmeyer, B. *NMR Basic Principles and Progress*; Springer-Verlag: New York, 1978; Vol. 14: Nuclear Magnetic Resonance Spectroscopy of Boron Compounds, Tables XI and XII, pp 136–139.

(11) Suginome, M.; Uehlin, L.; Yamamoto, A.; Murakami, M. *Org. Lett.* **2004**, *6*, 1167.

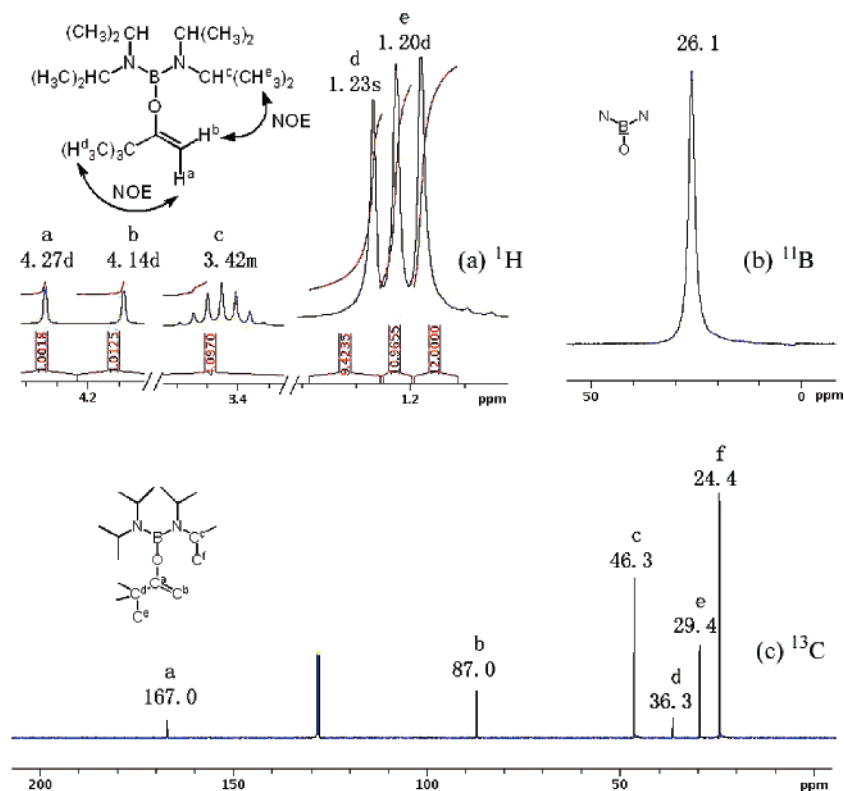


**Figure 3.** NMR spectra of bisaminoboron enolate. (a)  $^1\text{H}$  NMR (300 MHz,  $\text{C}_6\text{D}_6$ ): Proton  $\text{H}^a$  (4.27 ppm) shows an NOE with a *tert*-butyl group (1.23 ppm); Proton  $\text{H}^b$  (4.14 ppm) shows an NOE with *i*Pr groups (1.20 ppm). (b)  $^{11}\text{B}$  NMR (95 MHz,  $\text{C}_6\text{D}_6$ ). (c)  $^{13}\text{C}$  NMR (75 MHz,  $\text{C}_6\text{D}_6$ ): the chemical shift for tertiary carbon  $\text{C}^a$  (167.0 ppm) and methylene carbon  $\text{C}^b$  (87.0 ppm) is in agreement with other metal enolates.

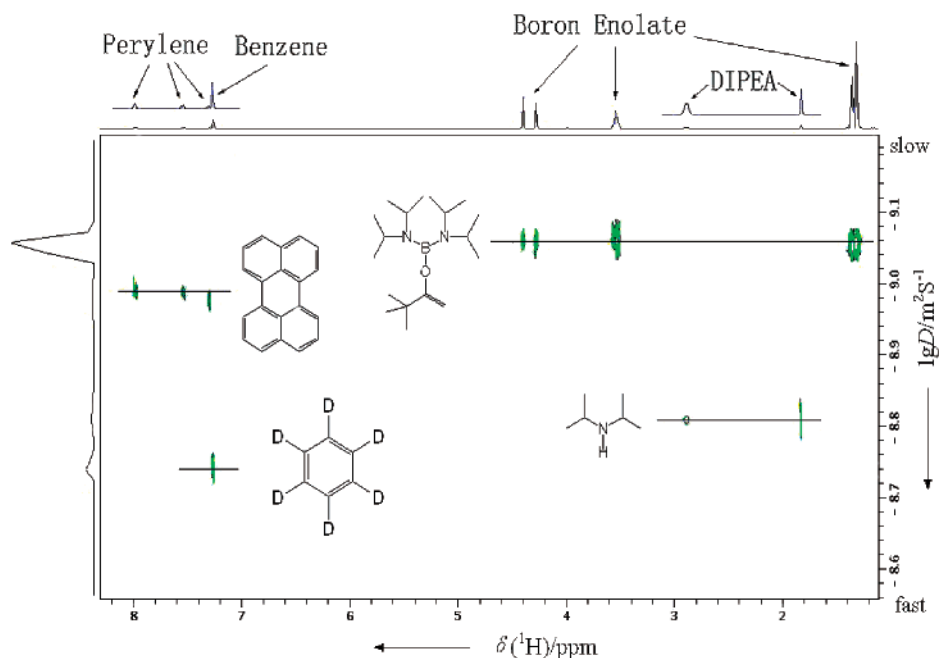


**Figure 4.** DOSY  $^1\text{H}$  NMR ( $\text{C}_6\text{D}_6$ , 400 MHz) of boron enolate, perylene, DIPEA, and benzene- $d_6$ . The diffusion coefficients calculated from the Stejskal–Tanner equation,  $\ln(I/I_0) = -[\gamma^2 \delta^2 (\Delta - \delta/3)] D \cdot G^2$ , are  $8.796 \times 10^{-10}$ ,  $1.043 \times 10^{-9}$ ,  $1.575 \times 10^{-9}$ , and  $1.860 \times 10^{-9} \text{ m}^2 \cdot \text{s}^{-1}$  respectively.  $I$  is the peak area,  $I_0$  is the peak area in the absence of gradients,  $\gamma$  is the magnetogyric ratio of the observed nucleus,  $\delta$  is the gradient duration,  $G$  is the strength of the gradient pulse in  $\text{T/m}$ ,  $\Delta$  is the diffusion time, and  $D$  is the diffusion coefficient.

that exhibited a NOE with vinylic proton b (see Figure 3). Although it is possible that the NMR spectra derive from a THF solvated species because the solvent utilized for these NMR experiments was a deuterated THF/freon mixture, we suggest that solvation of the boron complex by THF is not observed by NMR and that the chemical shift differences are a consequence

of the structural features of this enolate complex. Additionally, the diffusion-oriented NMR spectra exhibit no evidence of THF solvates.

We also determined the rotational barrier of the enolate **4b** to be  $7.38 \text{ kcal} \cdot \text{mol}^{-1}$  in keeping with the expected greater steric hindrance to rotation of the methyl-substituted enolate.

The most commonly used enolate forming boron reagents in organic synthesis include dibutylboron triflate and dicyclohexylboron chloride, which favor *Z*- and *E*-boron enolates, respectively. Initially we chose amino substituents, such as hexamethyldisilazane (HMDS), diisopropylamine (DIPA), and diethylamine, because the resultant bisaminoboron enolates are more stable in the solid state. As illustrated by others, bisaminoboron enolates are used to effect aldol reactions and produce  $\beta$ -amino carbonyl compounds in a Mannich-type reaction.<sup>17</sup> The ratio of these products is controlled by temperature, solvent, and substituents.

## Conclusion

In summary, we described the synthesis of bisaminoboron enolates and structure investigations of compound **3b**. This study addresses the resonance and steric effects on formation of bisaminoboron enolates. Taking all the experimental and theoretical investigations into consideration, it can be concluded that the greater reactivity observed for  $(i\text{Pr}_2\text{N})_2\text{BCl}$  is a compromise between the boron–nitrogen resonance and the nitrogen substituent steric effect. In addition, the structure and aggregation states of **3b** were investigated by X-ray crystallography and diffusion-ordered NMR techniques. It is important to point out that bisaminoboron enolate **3b** exists exclusively as monomer in both the solid state and solution states, indicating the boron center is open to coordinate to an incoming Lewis base. The methodology employed here is extendable to additional boron enolate systems. Investigations of the transition states in formation and subsequent reactions of boron enolates are currently in progress.<sup>18</sup>

## Experimental Section

**General.** All reactions were conducted under Ar atmosphere in flame-dried glassware under vacuum equipped with magnetic stirring bars. Ketones were purified by distillation over  $\text{CaCl}_2$  before use. THF was purified by a solvent-dispensing system. Anhydrous heptane was purchased from Aldrich.  $\text{BCl}_3$  was converted to  $\text{Me}_2\text{S}\cdot\text{BCl}_3$  for easier handling.  $\text{CF}_2\text{Cl}_2$  was purchased from SynQuest. IR spectra were recorded on a Perkin-Elmer 1600 series FTIR.

**NMR Measurements.**  $^1\text{H}$ ,  $^{13}\text{C}$ , and  $^{11}\text{B}$  NMR spectra were recorded on a Bruker DRX spectrometer. The spectra were recorded in  $\text{C}_6\text{D}_6$  at room temperature.  $\text{C}_6\text{D}_6$  solvent peaks were used as internal standard for  $^1\text{H}$  NMR (7.15) and  $^{13}\text{C}$  NMR (128.02).  $(\text{CH}_3\text{-CH}_2)_2\text{O}\cdot\text{BF}_3$  was used as external standard for  $^{11}\text{B}$  NMR; negative values are downfield from the standard. Data are reported as follows: chemical shift, multiplicity (s = singlet, d = doublet, t = triplet, q = quartet, h = heptet, br = broad, m = multiplet), coupling constants (Hz). DEPT135, HSQC, and NOESY NMR spectra were collected on a Bruker DRX-400 instrument equipped with an Accustar z-axis gradient amplifier and a QNP probe with a z-axis gradient coil. For the diffusion-ordered NMR (DOSY), the LEDbpgp2s pulse sequence was used. The pulse-field gradients ( $g$ ) were incremented in 64 steps from 2% to 95% of the maximum gradient strength in a linear ramp. A gradient length  $\delta$  of 1 ms ( $P30 = 0.5$  ms), a diffusion time  $\Delta$  of 0.2 s ( $D20$ ), and an eddy current delay of 5 ms ( $D21$ ) were employed. The diffusion

coefficient was determined by fitting the peak areas to the Stejskal–Tanner equation. For the low-temperature NMR, a mixture of boron enolate:THF- $d_8$ : $\text{CF}_2\text{Cl}_2 = 20\%:20\%:60\%$  was prepared. The sample was degassed and sealed in a heavy-wall NMR tube (Wilmad 522-PP-7) using a torch. Sample temperature was controlled using a Bruker Eurotherm 3300 temperature controller and a liquid nitrogen/nitrogen gas heat exchanger. Sample temperature was calibrated with a standard methanol sample.

**X-ray Structure Determinations.** Single crystals of **3b** suitable for X-ray diffraction studies were grown from heptane at low temperature. Crystallographic data and details of the refinement are summarized in Table 3. Crystallographic calculations were carried out using SHELXTL. Crystals were collected on a Bruker Smart Apex I diffractometer. The structure was solved from direct methods and Fourier syntheses and refined by full-matrix least-squares procedures with anisotropic thermal parameters for all non-hydrogen atoms. Hydrogen atoms bonded to carbon atoms were included in calculated positions ( $\text{C-H } 0.98 \text{ \AA}$ ) and refined riding on their attached atom. CCDC-647918 contains the supplementary crystallographic data for this paper.

**General Procedure for Preparation of Bisaminoboron Enolates. Using Lithium Enolates.** To a solution of diisopropylamine (DIPA) (6.8 mmol) in THF (6 mL) was added *n*-butyllithium (6.4 mmol, 2.42 M solution in hexanes) under an argon atmosphere at  $-20^\circ\text{C}$  and stirred for 30 min. The reaction mixture was then added dropwise the solution of ketone (6.2 mmol) in THF (1 mL). After stirring at  $-20^\circ\text{C}$  for an additional 30 min, a solution of chlorobis(dialkylamino)borane (6 mmol) in THF (2 mL) was added to the reaction mixture and stirred at room temperature for 24 h. The resulting solution was subject to centrifuge, and the LiCl precipitate was filtered. Evaporation of the volatile solvents followed by vacuum removal of diisopropylamine gave the crude product, which was purified by distillation or crystallization.

**Using Sodium or Potassium Enolates.** To a solution of sodium hexamethyldisilazane (NaHMDS) or potassium hexamethyldisilazane (KHMDS) (21 mmol) in THF (15 mL) was added ketone (20.5 mmol) in THF (2 mL) dropwise at  $0^\circ\text{C}$  under an argon atmosphere for 30 min. A solution of chlorobis(dialkylamino)borane (20 mmol) in THF (10 mL) was added to the reaction mixture and stirred at room temperature or  $60^\circ\text{C}$  for 1–12 h. The resulting solution was subject to centrifuge, and the NaCl or KCl precipitate was filtered. Evaporation of the volatile solvents followed by vacuum removal of HMDS gave the crude product, which was further purified by distillation or recrystallization.

**Bis(diethylamino)boron Enolate 3a.** Isolated yield: 3.66 g, 14.4 mmol, 72%. Bp  $90^\circ\text{C}/0.5$  mmHg.  $^1\text{H}$  NMR (300 MHz,  $\text{C}_6\text{D}_6$ ): 0.95 (s, 9H), 1.05 (triplet,  $J = 7.0$  Hz, 12H), 2.86–2.98 (q,  $J = 7.0$  Hz, 8H), 4.05 (d,  $J = 0.7$  Hz, 1H), 4.09 (d,  $J = 0.7$  Hz, 1H) ppm.  $^{13}\text{C}$  NMR (100 MHz,  $\text{C}_6\text{D}_6$ ): 15.1, 19.2, 40.5, 46.0, 87.6, 156.8 ppm.  $^{11}\text{B}$  NMR (96 MHz,  $\text{C}_6\text{D}_6$ ):  $-24.4$  ppm.

**Bis(diisopropylamino)boron Enolate 3b.** Isolated yield: 5.21 g, 16.8 mmol, 84%. It is very sensitive and readily hydrolyzes in air. Bp  $105^\circ\text{C}/0.5$  mmHg.  $^1\text{H}$  NMR (300 MHz,  $\text{C}_6\text{D}_6$ ): 1.20 (d,  $J = 6.9$  Hz, 24H), 1.24 (s, 9H), 3.38–3.47 (heptet,  $J = 6.6$  Hz, 4H), 4.14 (d,  $J = 0.8$  Hz, 1H), 4.27 (d,  $J = 0.8$  Hz, 1H) ppm.  $^{13}\text{C}$  NMR (75 MHz,  $\text{C}_6\text{D}_6$ ): 24.4, 29.4, 36.3, 46.3, 87.0, 167.0 ppm.  $^{11}\text{B}$  NMR (95 MHz,  $\text{C}_6\text{D}_6$ ):  $-26.1$  ppm.

**Bis(diisopropylamino)boron Enolate 4b.** Isolated yield: 5.18 g, 16.0 mmol, 80%. Bp  $120^\circ\text{C}/0.2$  mmHg.  $^1\text{H}$  NMR (400 MHz,  $\text{C}_6\text{D}_6$ ): 1.12 (s, 9H), 1.19 (d,  $J = 6.6$  Hz, 24H), 1.59 (d,  $J = 6.9$  Hz, 3H), 3.44–3.53 (heptet,  $J = 6.8$  Hz, 4H), 4.54 (quartet,  $J = 6.9$  Hz, 1H ppm).  $^{13}\text{C}$  NMR (100 MHz,  $\text{C}_6\text{D}_6$ ): 12.5, 23.8, 28.5, 35.6, 45.4, 94.6, 157.9 ppm.  $^{11}\text{B}$  NMR (96 MHz,  $\text{C}_6\text{D}_6$ ):  $-25.6$  ppm.

**Acknowledgment.** This work was supported by PHS–NIH GM-35982 and by the NSF CHE-0718275.

(17) (a) Suginome, M.; Uehlin, L.; Murakami, M. *J. Am. Chem. Soc.* **2004**, *126*, 13196. (b) Corey, E. J.; Huang, H. C. *Tetrahedron Lett.* **1989**, *30*, 5235. (c) Hoffmann, R. W.; Ditrich, K.; Froech, S. *Liebigs Ann. Chem.* **1987**, *977*. (d) Hoffmann, R. W.; Ditrich, K.; Froech, S.; Cremer, D. *Tetrahedron* **1985**, *41*, 5517.

(18) Preliminary results were presented: Ma, L.; Williard, P. G. *Abstracts of Papers*, 233rd ACS National Meeting, Chicago, IL, M 25–29, 2007; American Chemical Society: Washington, DC, 2007; ORGN-779.

**Supporting Information Available:** Cartesian coordinates of  $(\text{Et}_2\text{N})_2\text{BCl}$ ,  $(i\text{Pr}_2\text{N})_2\text{BCl}$ ,  $(\text{TMS}_2\text{N})_2\text{BCl}$ , **3b**, and perylene; X-ray crystal structure of **3b** in CIF format. This material is available free of charge via the Internet at <http://pubs.acs.org>. Crystallographic data have also been deposited with the Cambridge Crystallographic

Data Centre: CCDC-647918 (**3b**). Copies of the data can be obtained free of charge on application to CCDC, 12 Union Road, Cambridge CB2 1EZ, UK (fax: (+44)-1223-336-033; e-mail: [deposit@ccdc.cam.ac.uk](mailto:deposit@ccdc.cam.ac.uk)).

OM700676W